# SHAPE EFFECT OF CERIA ON THE ACTIVITY OF Au/$CeO_2$ FOR PREFERENTIAL CO OXIDATION

*Mike Carltonbird* [a], *Apanee Luengnaruemitchai* [a]

[a] The Petroleum and Petrochemical College, Chulalongkorn University

Keywords: Gold/Ceria, Shape effect, PROX

## ABSTRACT

Hydrogen is an energy carrier and considered as the main source for on-board hydrogen in Proton Exchange Membrane Fuel Cell applications. However, the anode of fuel cells can be poisoned by carbon monoxide (CO) in hydrogen stream produced from reforming of methanol reaction. Ceria ($CeO_2$) has been regarded as an interesting support for many reactions including preferential CO oxidation due to its unique properties. The morphology of ceria is one of the important factors that significantly affects the properties such as reactive exposed-crystal plane for reaction, surface area and oxygen storage capacity (OSC) including metal dispersion of catalyst. Gold-based catalyst has been considered as a potential catalyst for preferential CO oxidation. Recently, it was reported that the catalytic activity of Au catalysts strongly depended on the shape of ceria. In the present work, hydrothermal method was used to synthesize ceria in different shapes. The effect of ceria (rod, cube, polyhedron, and octahedron) morphology was investigated and characterized by many techniques.

***apanee.l@chula.ac.th**

## INTRODUCTION

The high demand for clean energy triggers the intensive interest in fuel cell-powered systems for stationary and mobile source applications because of their theoretical high fuel efficiency and low environmental impact. Numerous types of fuel cells have already been developed. Among them, one of the most promising is the proton exchange membrane fuel cell (PEMFC) fueled with hydrogen. Hydrogen is usually produced by steam reforming, autothermal reforming, or partial oxidation of natural gas, light oil fractions, and alcohols. Unfortunately, a noticeable amount of CO 5-15% is formed together with $H_2$, $H_2O$, and $CO_2$. This amount of CO has to further processed in a water gas shift reactor, resulting in low concentration of CO (0.5-1 %) (Wootsch *et al.*, 2004). However, depending on the type of anode of fuel cell, the CO concentration in the hydrogen feed must be less than 1-100 ppm. At this need, it leads to the developing in the PROX process which can remove CO concentration to below 10 ppm. In the last few years, an intense research effort to develop catalysts which can be able to selectively oxidize CO in the presence of excess $H_2$. Several catalytic systems have been tested in the PROX reaction and the most extensively studied is gold/ceria catalyst. The objective of this research is to study the effects of crystal plane and shape exposed on Au/$CeO_2$ catalysts, which influence on the catalytic activity for PROX of CO. The main variables in the present work are hydrothermal reaction temperature, and concentration of the starting material during support preparation. The ceria support were prepared by hydrothermal method. The Au/ $CeO_2$ catalysts were prepared by Deposition-Precipitation (DP) technique and characterized by X-ray Diffraction (XRD), Scanning

Electron Microscopy (SEM), BET Surface Area Measurement, Temperature-Programmed Reduction (TPR), and X-ray Photoelectron Spectroscopy (XPS).

## EXPERIMENTAL

### *A. Preparation of $CeO_2$ Support*

Sodium hydroxide or sodium phosphate was dissolved in DI water. Next, the homogeneous solution was formed under stirring. After that, the $Ce(NO_3)_3 \cdot 6H_2O$ precursor was added into the mixed solution, which was transferred into a 125 mL teflon-lined stainless steel autoclave later. Subsequently, the autoclave was laid in the oven at 100 °C, 170 °C, or 180 °C for 24 hours. The prepared products were washed with deionized water to eliminate excess ion and dried in the oven at 100 °C for 24 hours. The final products were obtained by calcination in air at 400 °C for 4 hours (Hu *et al*., 2016).

### *B. Preparation of $Au/CeO_2$ Catalyst*

For gold deposition, the desired amount of Hydrogen tetrachloroaurate (III), $HAuCl_4$, was dissolved in deionized water under continuous stirring, and then the dried support was suspended in a solution, which was adjusted the pH of solution ~8.5 by using 0.1 M $(NH_4)_2CO_3$. Subsequently, the mixture was kept at this pH for 1 hour. The suspension was washed by deionized water to remove the residue ions. Deionized precipitate was dried at 80 °C overnight and calcined in air at 400 °C for 4 hours (Zhang *et al*., 2014).

### *C. Catalytic Activity Measurement*

The PROX reaction was carried out in a fixed-bed reactor under atmospheric pressure and reaction temperatures were varied from 10 to 130 °C. The activity and selectivity of the $Au/CeO_2$ catalysts prepared at different conditions were obtained. Accordingly, important parameters during the catalyst preparation were investigated in order to correlate with the characterization results.

## RESULTS AND DISCUSSION

### *A. Structural Properties*

The scanning electron microscope (SEM) was employed for observe the morphology of the prepared $CeO_2$ supports and $Au/CeO_2$ catalysts. $CeO_2$ nanorod, nanocube, nanopolyhedra and nanooctahedra were selectively obtained by using $Ce(NO_3)_3$ as the cerium source with changing the base concentration ($C_{NaOH}$), base type (NaOH or $Na_3PO_4$) and hydrothermal temperature (T). Figure 1a shows $CeO_2$ nanorod was obtained by 6M NaOH prepared at 100 °C, while $CeO_2$ nanocube was formed at higher temperature (180 °C) with the same NaOH concentration, as shown in Figure 1c. For $CeO_2$ nanopolyhedra morphology was received by using low NaOH concentration, 0.1M NaOH prepared at 180 °C, and $CeO_2$ nanooctahedra was received by changing base type and hydrothermal temperature from NaOH to 0.01M $Na_3PO_4$ at 170 °C, as demonstrated in Figure 1e and 1g, respectively. While the SEM images of $Au/CeO_2$ nanorod, nanocube, nanopolyhedra and nanooctahedra catalysts are shown in Figure 1b, d, f, and h, respectively.

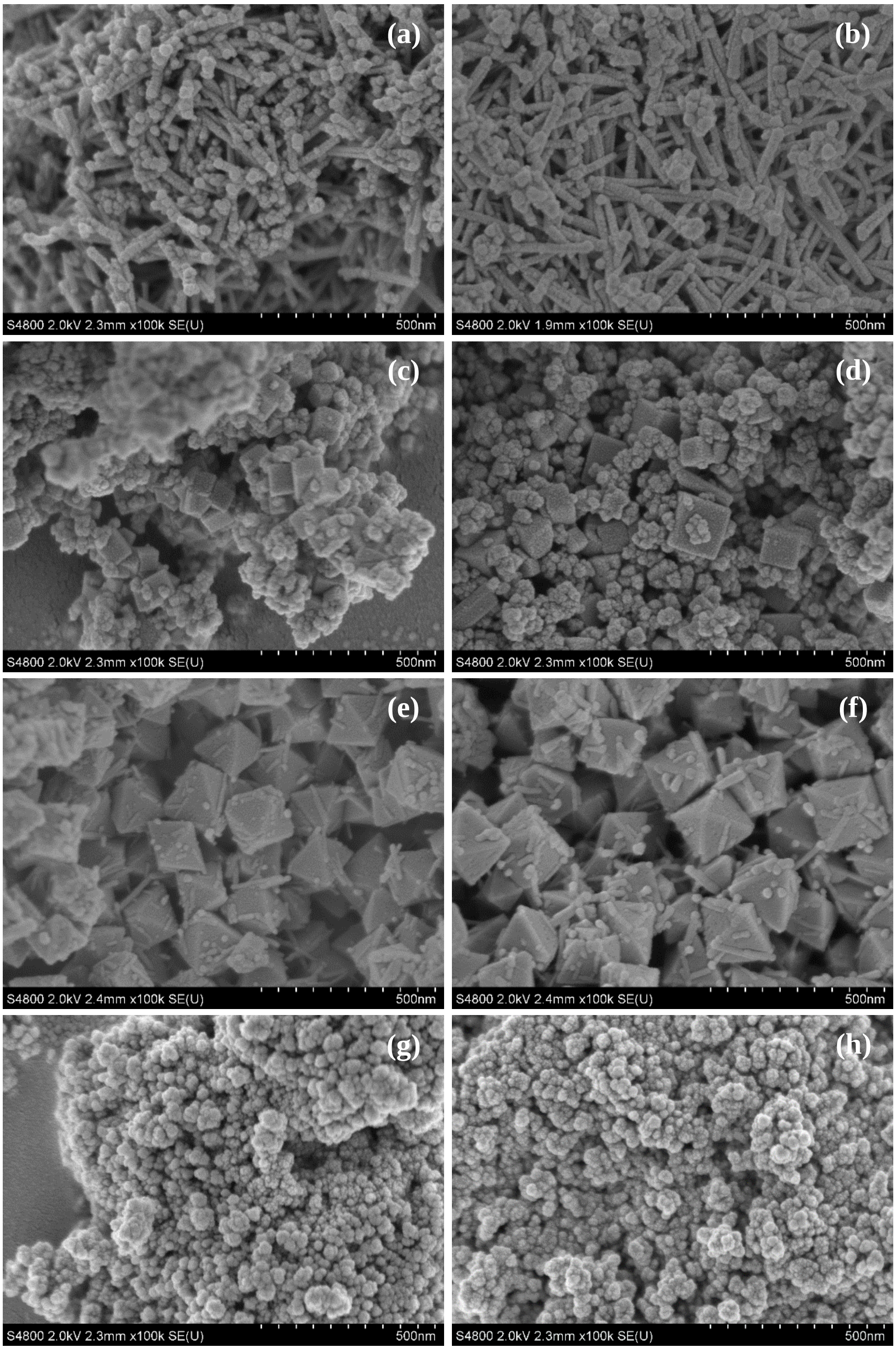

**Figure 1** SEM images of $CeO_2$ supports with various shapes, (a) nanorod, (c) nanocube, (e) nanopolyhedra, and (g) nanooctahedra and $Au/CeO_2$ catalysts with various shapes, (b) nanorod, (d) nanocube, (f) nanopolyhedra, and (h) nanooctahedra.

X-ray diffractometer was employed to analyze the crystalline structure of $Au/CeO_2$ catalysts and the mean crystallite size. The XRD patterns of $Au/CeO_2$ showed the fluorite cubic structure of $CeO_2$ by diffraction peaks, corresponding to (111), (200), (220), (311), (222), (400), (331), and (420), as shown in Figure 2. The mean crystallite size of $CeO_2$ was calculated from the half-width of (111) diffraction peak based on Scherrer's equation. Table 1 summarizes the crystallite sizes of Au/$CeO_2$ with various shapes.

There is no diffraction peak of gold crystalline appeared in all XRD patterns, which is probably due to very small size of gold particles and/or fine dispersion of gold on the surface of support. Moreover, the XRD pattern of Au/$CeO_2$ nanooctahedra exhibits sharp peaks and high intensity, which indicate large $CeO_2$ crystallites and relatively high ordered structure existing, as shown in Figure 2.

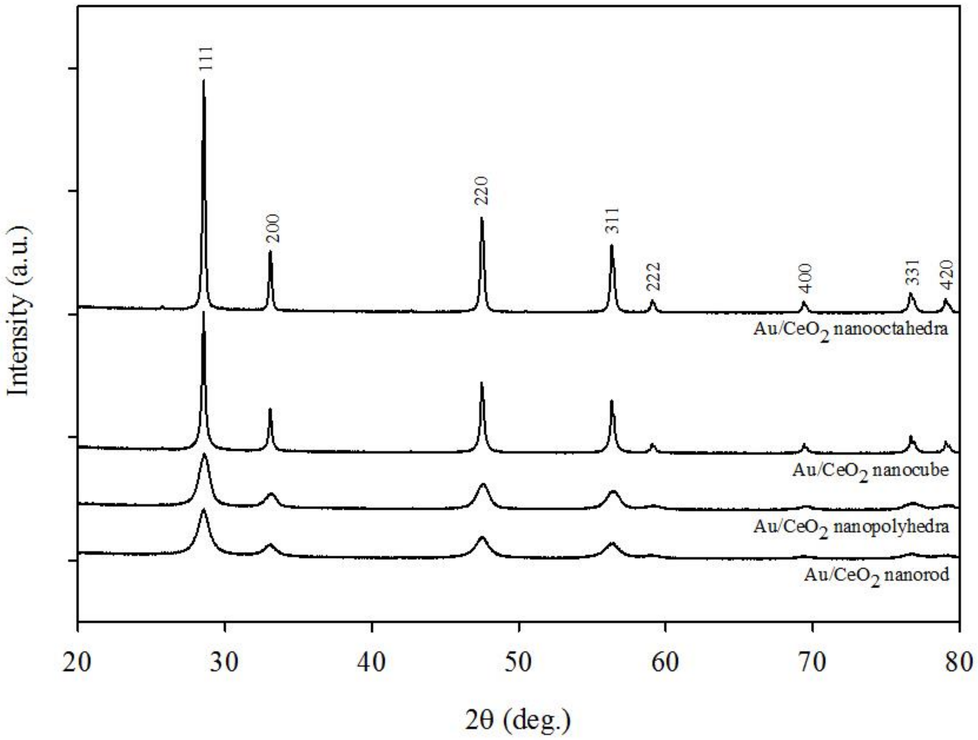

**Figure 2** XRD patterns of Au/$CeO_2$ catalysts with various shapes.

**Table 1** Crystallite size, BET surface area, total pore volume, and average pore diameter of investigated adsorbents

| Sample | Physical characterization | | | |
|---|---|---|---|---|
| | Crystallite size* (nm) | BET surface area ($m^2/g$) | Total pore volume ($cm^3/g$) | Average pore diameter (nm) |
| Rod | 18.08 | 93.9 | 0.6696 | 28.51 |
| Cube | 89.07 | 27.4 | 0.2265 | 33.08 |
| Octahedra | 100.97 | 6.9 | 0.2414 | 139.40 |
| Polyhedra | 20.28 | 92.7 | 0.2509 | 10.83 |
| 1%wt Au-Rod | 19.01 | 93.4 | 0.6198 | 26.53 |
| 1%wt Au-Cube | 89.61 | 26.8 | 0.2748 | 40.95 |
| 1%wt Au-Octahedra | 101.63 | 6.5 | 0.1888 | 117.00 |

| | | | | |
|---|---|---|---|---|
| 1%wt Au-Polyhedra | 20.45 | 91.5 | 0.2280 | 9.97 |

* Calculated from the half-width of (111) diffraction peak based on Scherrer's equation.

Autosorb-1MP Gas Sorption System (Quantachrome Corparation) was used to measure BET surface area, total pore volume, and average pore diameter of the prepared catalysts. The surface area measurement was analyzed from nitrogen adsorption-desorption isotherm. BET surface area, pore volume, and average pore diameter were listed in Table 1. $CeO_2$ nanorod has relatively high surface area (93.9 $m^2/g$) and small pore diameter (28.51 nm), while $CeO_2$ nanooctahedra has the lowest surface area of 6.9 $m^2/g$ and the highest pore diameter (139.40 nm), which is consistent with the crystallite size obtained from XRD results. After loading 1%wt Au onto $CeO_2$ supports, the specific surface area are slightly reduced because of the deposition of Au on the $CeO_2$ surface structure.

*B. Catalytic Performance*

Figure 3. shows the activity of Au/$CeO_2$ catalysts with various shapes for PROX reaction. Au catalyst supported on Rod shape ceria has the highest activity of 97.9 % at 30 °C, followed by Au catalyst supported on Polyhedra shape ceria 94.0 % at 50 °C, Au catalyst supported on Cube shape ceria 74.0 % at 70 °C, and Au catalyst supported on Octahedra shape ceria 27.7 % at 70 °C, respectively. These results indicate that the shape of $CeO_2$ support has significantly impact on the catalytic activity of CO oxidation.

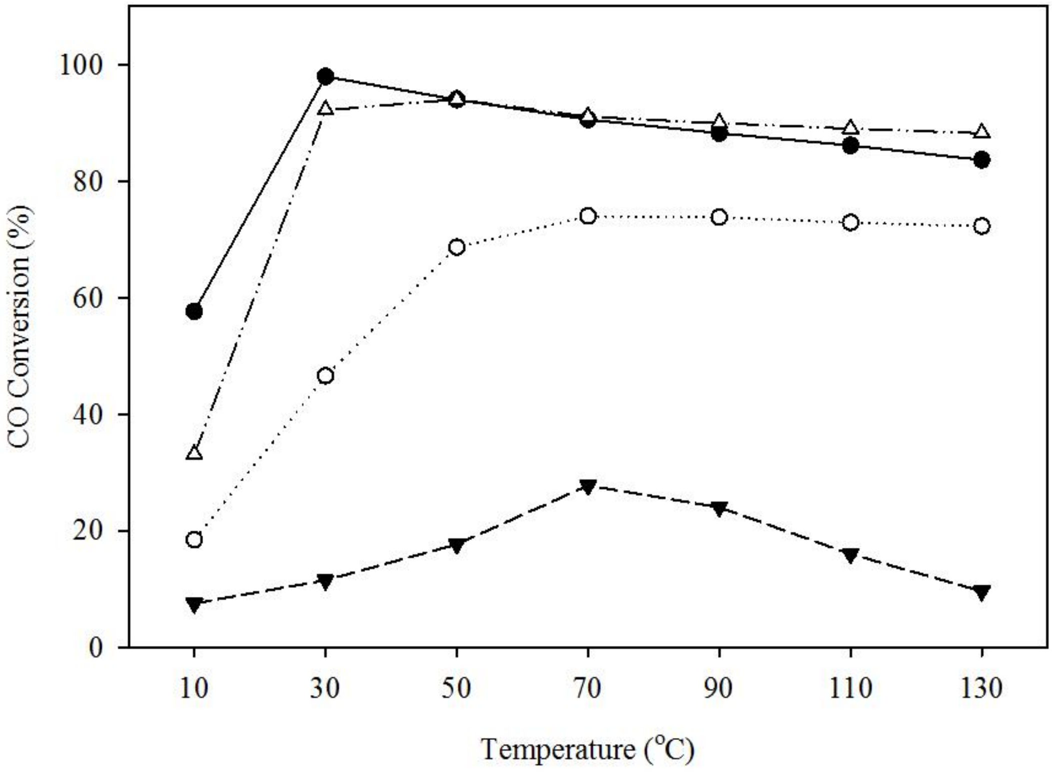

**Figure 3** CO conversion activity of (●) Au-Rod, (○) Au-Cube, (▼) Au-Octahedra, and (Δ) Au-Polyhedra.

## CONCLUSIONS

The results in this study indicate that the specific surface area of $CeO_2$ plays an important role in catalytic activity of $Au/CeO_2$. The morphology of ceria has been observed, based on the results, it shows that not only the $CeO_2$ crystallite size, but also surface structure are important for achieving high catalytic activity of $Au/CeO_2$ catalyst. Among the samples studied. $Au/CeO_2$ rod shape gives the highest activity due to its small crystallite size and high surface area, followed by polyhedral shape, cube shape, and octahedral shape, respectively.

## ACKNOWLEDGEMENTS

The authors would like to sincerely thank for the scholarship and funding of this thesis work provided by the Petroleum and Petrochemical College, and the Methee-Vijai-Chula Grant; Grant for International Research Integration.

## REFERENCES

**Chen, L., Wang, S., Chen, C., and Zhang, N.** (2011). Transition Metal Chemistry, 36(4), 387-393.
**Deng, W., Jesus, J. D., Saltsburg, H., and Flytzani-Stephanopoulos, M.** (2005). Applied Catalysis A: General, 291(1–2), 126-135.
**Hu, Z., Liu, X., Meng, D., Guo, Y., Guo, Y., and Lu, G.** (2016). ACS Catalysis, 6(4), 2265-2279.
**Huang, X.-S., Sun, H., Wang, L.-C., Liu, Y.-M., Fan, K.-N., and Cao, Y.** (2009). Applied Catalysis B: Environmental, 90(1–2), 224-232.
**Radnik, J., Wilde, L., Schneider, M., Pohl, M. M., and Herein, D.** (2006). The Journal of Physical Chemistry B, 110(47), 23688-23693.
**Schubert, M. M., Plzak, V., Garche, J., and Behm, R. J.** (2001). Catalysis Letters, 76(3), 143-150.
**Wang, S., Zhao, L., Wang, W., Zhao, Y., Zhang, G., Ma, X., and Gong, J.** (2013). Nanoscale, 5(12), 5582-5588.
**Wang, X., Jiang, Z., Zheng, B., Xie, Z., and Zheng, L.** (2012). CrystEngComm, 14(22), 7579-7582.
**Zhang, S., Li, X.-S., Chen, B., Zhu, X., Shi, C., and Zhu, A.-M.** (2014). ACS Catalysis, 4(10), 3481-3489.